

Sliding Mode Reference Conditioning Force Constraint Mechanism for Closed-loop Wave Energy Controllers

Pedro Fornaro^{1,2}

¹*Centre for Ocean Energy Research*
National university of Ireland, Maynooth
Maynooth, Co. Kildare, Ireland
pedro.fornaro@mu.ie

Pablo E. Muñoz²

²*GECEP, Instituto LEIC,*
UNLP-CONICET, La Plata, Argentina
pablo.munoz@ing.unlp.edu.ar

Sergio A. González²

²*GECEP, Instituto LEICI,*
UNLP-CONICET, La Plata, Argentina
sag@ing.unlp.edu.ar

Paul F. Puleston²

²*GECEP, Instituto LEICI,*
UNLP-CONICET, La Plata, Argentina
puleston@ing.unlp.edu.ar

John V. Ringwood¹

¹*Centre for Ocean Energy Research*
National university of Ireland, Maynooth
Maynooth, Co. Kildare, Ireland
john.ringwood@mu.ie

Abstract—Wave energy converters (WEC) are structures capable of harnessing the energy from waves. Since WECs are deployed in the ocean, control system technologies play a fundamental role in guaranteeing safe and reliable operation, by keeping WECs operating within their physical constraints. However, to date, there are no effective real-time force constraint mechanisms (capable of dealing with model uncertainty), which is prohibitive for implementation. In this paper, by employing a Sliding Mode (SM)-based reference conditioning (SMRC) technique, a (causal) force constraint method for WECs is designed. To effectively implement the force constraint algorithm, a position-tracking architecture is required. In this control structure, the position reference is provided by an outer loop, based on spectral control for WECs, while the internal loop is an internal model-based tracking controller. Finally, numerical results show that SMRC is effectively capable of robustly satisfying force constraints, even in the presence of WEC modelling uncertainty.

Keywords—Wave energy systems, reference conditioning, optimal control.

I. INTRODUCTION

The necessity to speed up the energy transition is undebatable. While most of the focus and attention have been drawn to the more conventional wind and solar technologies, alternative sources of renewable energy are fundamental to contribute to the energy mix. This is because the integration of multiple sources of renewables reduces production variability and enhances system stability, resilience, and grid penetration. In particular, with a global annual potential estimated between 1 and 10 TWh [1], wave energy converters (WEC), represent a promising renewable energy technology. Despite its promise, high capital and operational costs associated with deployment in the harsh ocean environment hinder the large-scale commercialisation of wave energy converters (WEC) [2].

A crucial step toward the commercial viability of WECs is implementing energy-maximising control systems, which ensure maximal power extraction while managing operational

constraints to protect the device from damage [3]. Specifically, position and force (alternatively, torque) constraints must be satisfied for a broad set of operational conditions. Common optimisation-based (OB) controllers, such as model predictive control (MPC), spectral methods (SPC) [4], and moment-based (MBC) algorithms [3] [5], provide, by resorting to numerical routines, constrained energy-maximising solutions. However, model mismatch and/or unmodelled dynamics affect the performance of OB controllers, since (i) with the exception of MPC, OB controllers use a feed-forward structure to implement the optimal control force, and (ii) for the design of OB controllers, a restrictive set of WEC modelling assumptions are made. Hence, in practice, model mismatch or unmodelled dynamics may easily result in the violation of position and/or force constraints.

Satisfying the position constraints has been solved by employing velocity tracking control structures, such as in [6] [7]. This consists of closing the control loop to track the optimal velocity, inherently satisfying position constraints. However, the effects of non-ideal control actuators, uncertainty, and unmodelled dynamics, must be considered by using a different approach. Indeed, although considering a tracking structure may be sufficient to satisfy position constraints (even in the presence of model uncertainty), the tracking controller generates an *excess* of the control force to compensate for model mismatches, potentially leading to the violation of the control force constraints. Another alternative is using robust control techniques [8]; however, the introduced conservatism leads to a reduction in power absorption and increased computational complexity.

Motivated by the requirement of a robust real-time implementable force constraint mechanism for the WEC actuator, i.e., the power take-off (PTO) mechanism, this paper presents a sliding-mode (SM) reference conditioning (SMRC) mecha-

nism for WECs. The designed mechanism limits the control action without compromising the operation of the tracking controller [9]. The SMRC method operates by keeping the control force on a sliding surface, preventing the control effort from exceeding the specified constraint. Importantly, this mechanism is only operative when the control force approaches the constraint but does not affect the nominal operation conditions when the control effort is far from the constraint limits.

To design the SMRC method, a position tracking structure is required. In this control architecture, the position reference is provided by an open-loop spectral controller (SC), which operates as a supervisory outer loop. The SC provides an optimal control force and a position reference by employing a nominal WEC model, while the inner loop consists of an internal model-based controller (IMC) as in [10]. The presented results show that, unlike the SC controller case, in the presence of modelling uncertainty, without requiring optimisation or complex tuning, the SMRC mechanism guarantees safe operation, keeping the WEC within its physical constraints. Additionally, it is worth noting that a position-tracking structure is used for the inner tracking loop, as it is empirically shown that solely employing a velocity-tracking structure, in combination with the SMRC, results in critical violations of the position constraints.

This paper is organised as follows. Section II presents the WEC modelling and control fundamentals, together with the tracking structure employed in this paper. Then, Section III presents the SMRC method adapted for WECs, and results obtained using SMRC are presented in Section IV. Lastly, the main conclusions are drawn in Section V.

II. TRACKING CONTROL FOR WECs

In this Section, the WEC control strategy, based on a position tracking structure, is presented. To that end, first, the WEC modelling principles are presented in Subsection II-A. Then, Subsection II-B briefly presents and discusses the control fundamentals for WECs. Then, subsection II-C presents the position tracking control strategy.

A. Hydrodynamic WEC modelling fundamentals

WECs are floating bodies that oscillate with the reciprocating motion of waves; hence, typically, a mass-spring-damper model can be used to describe WEC dynamics (see [11]):

$$\underbrace{m}_{\text{Mass}} \dot{v}(t) = \underbrace{f_{ex}(t) + f_u(t)}_{\text{External forces}} - \underbrace{f_h(z)}_{\text{'Spring'}} - \underbrace{\tilde{f}_r(v, \dot{v})}_{\text{'Damping'}}, \quad (1)$$

where $z(t)$, $v(t)$, and $\dot{v}(t)$, represent the WEC displacement, velocity and acceleration, respectively. Also, m is the mass of the device, $f_{ex}(t)$ is the wave excitation force, $f_u(t)$ is the control force, $f_h(z) = k_z z(t)$, is the restoring force (with k_z being the ‘spring’ coefficient), and $\tilde{f}_r(v, \dot{v})$, is the radiation force defined [12] as:

$$\tilde{f}_r(t) = m_\infty \dot{v}(t) + \underbrace{\int_{t_0}^t h_r(t-\tau)v(\tau)d\tau}_{f_r(t)}, \quad (2)$$

where m_∞ is the infinite frequency asymptote of the radiation added-mass and $h_r(t)$ is the impulse response of the linear convolution operator, which describes the memory effect of the fluid response [13]. The convolution operator, $f_r(\cdot)$, describes a causal and passive system, and thus can be approximated as a linear, continuous-time, strictly proper, and finite-dimensional system:

$$\dot{\mathbf{z}}_r = \mathbf{F}\mathbf{z}_r + \mathbf{G}v, \quad (3a)$$

$$f_r \approx \mathbf{H}\mathbf{z}_r, \quad (3b)$$

with $\mathbf{F} \in \mathbb{R}^{n_r \times n_r}$, being Hurwitz, $\mathbf{G} \in \mathbb{R}^{n_r \times 1}$, and $\mathbf{H} \in \mathbb{R}^{1 \times n_r}$. Thus, $\mathbf{z}_r \in \mathbb{R}^{n_r}$. For a formal discussion on the properties of (3), see [13]. Considering (1)–(3), and assuming that the output is the measured position, a complete state space representation of the WEC dynamics is:

$$\dot{\mathbf{x}} = \mathbf{A}\mathbf{x} + \mathbf{B}(f_{ex} + f_u), \quad (4a)$$

$$v = \mathbf{C}\mathbf{x}, \quad (4b)$$

where $\mathbf{x}^\top = [z, v, \mathbf{z}_r^\top]$, and \mathbf{A} , \mathbf{B} , and \mathbf{C} are defined as:

$$\mathbf{A} = \begin{bmatrix} \mathbf{A}' & -\mathbf{B}'\mathbf{H} \\ \mathbf{G}\mathbf{C}' & \mathbf{F} \end{bmatrix}, \mathbf{B} = \begin{bmatrix} \mathbf{B}' \\ \mathbf{0} \end{bmatrix}, \mathbf{C}^\top = \begin{bmatrix} \mathbf{C}' \\ \mathbf{0} \end{bmatrix}, \quad (5)$$

with:

$$\mathbf{A}' = \begin{bmatrix} 0 & 1 \\ -\mathcal{M}k_z & 0 \end{bmatrix}, \mathbf{B}' = \begin{bmatrix} 0 \\ \mathcal{M} \end{bmatrix}, (\mathbf{C}')^\top = \begin{bmatrix} 1 \\ 0 \end{bmatrix}, \quad (6)$$

where $\mathcal{M} = (m + m_\infty)^{-1}$, and the zero vectors $\mathbf{0} \in \mathbb{R}^{n_r}$.

B. Control specifications

Typically, the WEC control problem is associated with extremising a cost function over an interval $T \in \mathbb{R}_+$, subjected to system constraints as:

$$\begin{aligned} f_u &= \arg \max_{f_u} \{ \mathcal{J}_T(f_u) \}, \\ &\text{s.t.} \\ &\text{System dynamics,} \\ &\text{Physical constraints.} \end{aligned} \quad (7)$$

where f_u is designed to extremise the cost function $\mathcal{J}_T(f_u)$. In this paper, for clarity sake, and without losing generality, it is assumed that $\mathcal{J}_T(f_u)$ is defined as the integral of converted mechanical power:

$$\mathcal{J}_T = - \int_T f_u v(\tau) d\tau. \quad (8)$$

Solving (7) provides an optimal control force, f_u^* , which, using the system dynamics, (4), gives the optimal system trajectories, $z^*(t)$, and $v^*(t)$. Then, $z^*(t)$ is used as a reference for the tracking controller, as detailed in Subsection II-C.

C. Position tracking architecture

The position tracking (PT) control structure used in this paper is presented in Figure 1. In essence, the PT structure requires a position reference, which is provided by an outer control loop that solves (7) (as detailed in the previous Subsection II-B), and a tracking structure capable of robustly tracking the provided reference. In the following, the employed outer and inner control loop are presented.

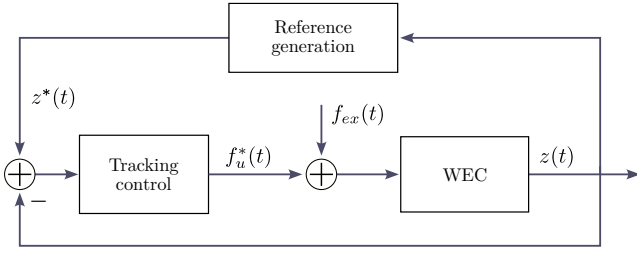


Figure 1. Illustrative diagram of a PT control loop for WECs.

1) *Outer loop*: The position reference may be obtained by solving (7) using different numerical approaches. In this paper, z^* is provided by an SC. This control solves, by resorting to numerical optimisation routines and using an estimate of the excitation force f_{ex}^1 , a solution for problem (7). In essence, the SC provides, for a nominal WEC model, a reference position z^* , and a control force f_u^* , which consider the constraints in (7). Hence, without model uncertainty, the control scheme from Figure 1 would inherently satisfy both position and force constraints.

2) *Inner loop*: In this paper, an internal model-based tracking control is employed for the low-level control loop. In the scheme from Figure 1, the main objective of IMC is to robustly track the velocity/position reference, even in the presence of WEC model uncertainty. IMC exploits the concept that, for stable processes, feedback is only necessary in the presence of model uncertainty. Following the design guidelines presented in [10], the IMC may be designed using the Youla–Kučera parametrisation, which provides the family of all stabilising controllers for system (4), parametrised by a proper rational stable transfer function $Q(s)$. Hence, let $G_0(s) = \mathbf{C}(s\mathbb{I} - \mathbf{A})^{-1}\mathbf{B}$, be the Laplace transfer function of the nominal system (4). Then, the family of all stabilising controllers $K(s)$, for $G_0(s)$, is given by:

$$C(s) = \frac{Q(s)}{1 - Q(s)G_0(s)}, \quad (9)$$

where $Q(s)$ is

$$Q(s) = \tilde{Q}(s)G_0^{-1}(s), \quad (10)$$

and $\tilde{Q}(s)$ a user-defined transfer function, designed considering that the stability of $Q(s)$ is necessary and sufficient to guarantee stability of the associated closed loop in Figure 1. Naturally, the selection of $Q(s)$ (equivalently, of $\tilde{Q}(s)$) is not unique. The approach used in this paper, is to design $\tilde{Q}(s)$ as:

$$\tilde{Q}(s) = \frac{1}{(1 + \frac{s}{\omega_c})^{n_c}}, \quad (11)$$

where ω_c defines a cut-off frequency, and n_c is the filter order. The user-defined variables, ω_c and n_c , are designed considering the trade-off between tracking performance and noise attenuation.

¹Note that, in Figure 1, the measured position is used as input in the reference generation block. This is because solving (7) requires an excitation force f_{ex} estimate, which is obtained via unknown input observers, as in [14], by using measurements of the WEC position and/or velocity.

III. SLIDING MODE REFERENCE CONDITIONING (SMRC)-BASED FORCE CONSTRAINT MECHANISM

Using the control scheme in Figure 1, the position constraints are satisfied by means of IMC control. Additionally, the IMC reference, obtained via SC control, inherently considers force constraints. However, in the presence of model uncertainty, tracking z^* may require large PTO control forces. As a result, considering model uncertainty, the control action f_u may violate the constraint:

$$|f_u(t)| \leq f_{max}. \quad (12)$$

Importantly, the latter problem has not been addressed in the wave energy control literature. Hence, in this section, a hard constraint mechanism that satisfies (12) $\forall t$, is presented. The method, based on SM, and applied to the PT control structure of WECs, is first presented in Section III-A and formalised in Section III-B.

A. SMRC fundamentals

In opposition to classic SM control, SMRC does not operate continuously, and SMRC only acts in a region defined by the constraints. Specifically, to satisfy constraint (12), when the control action reaches a sliding manifold, SMRC modifies the IMC reference. The rationale behind modifying the IMC reference is simple: A highly varying or large-amplitude reference profile results in large control efforts required to track such a profile. Therefore, to limit the operational space of the control force, the SMRC method reduces the reference profile z^* , when f_u approaches the constraints. In essence, the

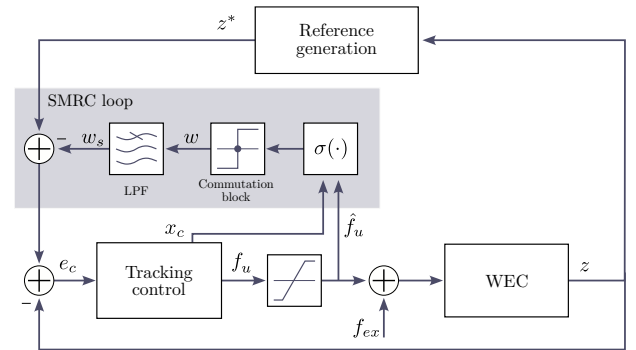


Figure 2. SMRC force constraint method applied to a PT control for WECs.

SMRC loop is composed of three subsystems (see Figure 2). (i) A user-defined switching function $\sigma(\cdot)$, (ii) a commutation block where a discontinuous action is implemented, and (iii) a low-pass filter (LPF), which provides a smooth output of the SMRC, w_s . Additionally, assume that the control force may be saturated, and define the saturated control force \hat{f}_u as:

$$\hat{f}_u = \begin{cases} f_{max} & \text{if } f_u > f_{max}, \\ f_u & \text{if } -f_{max} < f_u < f_{max}, \\ f_{min} & \text{if } f_u < -f_{max}. \end{cases} \quad (13)$$

The main objective of SMRC is to limit the control force f_u , between two surfaces, \bar{S} and \underline{S} , defined by the switching

function $\sigma(\cdot)$, and designed to ensure constraint (12). Formally, \bar{S} and \underline{S} are defined as:

$$\begin{aligned}\bar{S} &= \{x_c \in \mathcal{X}_c : \sigma |_{\hat{f}_u=f_{max}} = 0\}, \\ \underline{S} &= \{x_c \in \mathcal{X}_c : \sigma |_{\hat{f}_u=-f_{max}} = 0\}.\end{aligned}\quad (14)$$

where $x_c \in \mathcal{X}_c \subset \mathbb{R}^n$ is the IMC controller state. In words, by keeping the control variables between the surfaces defined by \bar{S} and \underline{S} , the controller operational space is limited to satisfy constraint (12). To force $\sigma = 0$, when the control force, f_u , approaches the constraint limits, the discontinuous signal, w ,

$$w = \begin{cases} w^+ & \text{if } \sigma < 0 \\ w^- & \text{if } \sigma > 0 \\ 0 & \text{if } \sigma = 0 \end{cases}\quad (15)$$

is implemented in the commutation block. An illustrative scheme of the SMRC operation is presented in Figure 3. Note

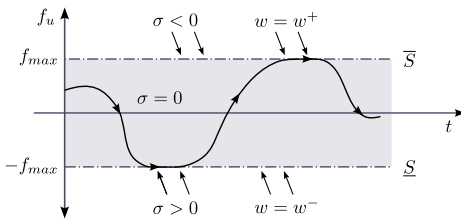


Figure 3. Graphical interpretation of the SMRC operation.

that, if x_c is between \bar{S} , \underline{S} , then $\sigma = 0$, $w = 0$, and the reference is not modified (SMRC is not active). However, when x_c reaches \bar{S} , or \underline{S} , w becomes nonzero, driving the control force to $\sigma = 0$, and preventing $f_u = C_c x_c$ from exceeding the specified constraints. For an effective operation of SMRC, the following conditions are required:

- (C1) **Transversality condition** [15]. The switching function σ is of unitary relative degree with respect to the discontinuous action ($\dot{\sigma}$ must be an explicit function of w),
- (C2) **Gain condition** [15]. The amplitudes w^+ , w^- , satisfy:

$$\begin{aligned}0 &< \underline{w}_{eq} < w^+ \\ w^- &< \bar{w}_{eq} < 0\end{aligned}\quad (16)$$

where \underline{w}_{eq} and \bar{w}_{eq} are *equivalent* continuous actions.

While w^+ , w^- , may be empirically selected to satisfy (C2), the relative degree condition, (C1), typically requires an analysis of the variables in the considered application.

B. Design of the SMRC for WECs

In this section, the SMRC operation conditions, (C1) and (C2), detailed in Subsection III-A, are used for the SMRC design for WECs. To that end, $\sigma(\cdot)$, and the LPF, are designed considering a PT closed-loop control (see Figure 2).

First, to verify (C1), the relative degree of f_u with respect to w is evaluated. To that end, the IMC controller, designed in Section II-C, is rewritten in state-space form as:

$$C(s) : \begin{cases} \dot{x}_c = A_c x_c + B_c e_c \\ f_u = C_c x_c, \end{cases}\quad (17)$$

where $x_c \in \mathcal{X}_c \subset \mathbb{R}^n$ is the controller state, $A_c \in \mathbb{R}^{n_c \times n_c}$ is the dynamic matrix, $B_c \in \mathbb{R}^{n_c \times 1}$ is the input matrix, and $C_c \in \mathbb{R}^{1 \times n_c}$ is the output matrix. Additionally, let:

$$e_c = z^* + w_s - z, \quad (18)$$

be the conditioned error, with w_s being the SMRC output, provided by a first-order LPF:

$$LPF : \begin{cases} \dot{x}_F = \lambda_F (w - x_F) \\ w_s = x_F, \end{cases}\quad (19)$$

with $\lambda_F > 0$. Typically, the IMC control is designed to satisfy *nominal* operational conditions. Hence, it is assumed that the control action f_u , is of relative degree ρ with respect to e_c . Then, the ρ -time derivative of f_u results:

$$f_u^{(\rho)} = C_c A_c^{(\rho)} x_c + C_c A_c^{(\rho-1)} B_c e_c, \quad (20)$$

with the first $(\rho - 1)$ Markov parameters identically null; i.e., $C_c B_c = C_c A_c B_c = \dots = C_c A_c^{(\rho-2)} B_c = 0$ and the ρ -th term $C_c A_c^{(\rho-1)} B_c \neq 0$. Hence, to satisfy (C1), considering (20), and that e_c is of relative degree one with respect to w (due to (19)), $\sigma(\cdot)$ must be a function of the ρ -time derivative of f_u . As a result, considering constraints (12), (19), and (20), the commutation function is designed as:

$$\sigma = \hat{f}_u - f_u - \sum_{\alpha=1}^{\rho} k_{\alpha} f_u^{(\alpha)} \quad (21)$$

where k_{α} are constant gains and $k_{\rho} \neq 0$. Note that (21) determines the allowed region

$$\mathcal{R} = \{x_c \in \mathcal{X}_c : \sigma = 0\}. \quad (22)$$

Thus, if $|f_u + \sum_{\alpha=1}^{\rho} k_{\alpha} f_u^{(\alpha)}|$ tends to exceed f_{max} , then $w \neq 0$, and (15) and (21) force $|f_u + \sum_{\alpha=1}^{\rho} k_{\alpha} f_u^{(\alpha)}|$ to remain in \mathcal{R} , modifying the reference z^* . In practice, z^* is conditioned before f_u reaches f_{max} , since the derivatives $|\sum_{\alpha=1}^{\rho} k_{\alpha} f_u^{(\alpha)}|$ introduces conservatism in the design of $\sigma(\cdot)$, in (21).

It is important to consider that the designed SMRC-based force constraint mechanism, is not active when $|f_u + \sum_{\alpha=1}^{\rho} k_{\alpha} f_u^{(\alpha)}| < f_{max}$. Subsequently, the SMRC method does not alter $z^*(t)$ in \mathcal{R} . Hence, the method satisfies optimality of the controlled WEC, in the sense defined in (7), when the SMRC mechanism is not active.

With respect to (C2), the values w^+ , and w^- , may be selected considering the infinity norm of the conditioned reference, i.e., $w^+ = w^- = \|z^*\|_{\infty}$. Complementary, w^+ , and w^- , may be empirically tuned by resorting to numerical evaluation.

IV. RESULTS AND DISCUSSION

In this section, to evaluate the SMRC performance, in-silico evaluations are conducted on a one-degree-of-freedom point absorber WEC. The simulation parameters are presented in Subsection IV-A. Then, velocity-tracking and position-tracking results are presented and compared in Subsection IV-B.

A. Preliminaries

First, to generate a realistic wave profile, the Bretschneider spectrum, considering a peak period $T_p = 8s$, and significant wave height $H_s = 1m$, is employed. Second, the SMRC is evaluated on a CorePower-like WEC device with parameters obtained from [16]. Then, by assuming linear hydrodynamics, and considering a one-degree-of-freedom device constrained to heave motion (movement in the z axis only), the WEC dynamics are given by (4), where \mathcal{M} and k_z are presented in Table I, the zero vectors are $\mathbf{0} \in \mathbb{R}^7$, and \mathbf{F} , \mathbf{G} , and \mathbf{H} are given by [16]:

$$\mathbf{F} = \begin{bmatrix} -7 & -24 & -47 & -57 & -43 & -18 & -3.4 \\ 1 & 0 & 0 & 0 & 0 & 0 & 0 \\ 0 & 1 & 0 & 0 & 0 & 0 & 0 \\ 0 & 0 & 1 & 0 & 0 & 0 & 0 \\ 0 & 0 & 0 & 1 & 0 & 0 & 0 \\ 0 & 0 & 0 & 0 & 1 & 0 & 0 \\ 0 & 0 & 0 & 0 & 0 & 1 & 0 \end{bmatrix}, \quad (23a)$$

$$\mathbf{G} = [1.46 \cdot 10^5 \ 0 \ 0 \ 0 \ 0 \ 0 \ 0]^T, \quad (23b)$$

$$\mathbf{H} = [0.21 \ 1.1 \ 3.8 \ 4.6 \ 3 \ 0.64 \ 0.014] \cdot 10^{-5}. \quad (23c)$$

Table I
NOMINAL WEC MODEL, CONTROL, AND SMRC PARAMETERS

WEC model parameters		
$\mathcal{M} = 6.8 \times 10^{-6}$	$k_z = 5.57 \times 10^5$	$n_r = 7$
PT control parameters		
Position constraint z_M	1.5 [m]	
Force constraint f_{max}	0.8 [N]	
IMC cut-off frequency ω_c	100 [rad/s]	
IMC filter order n_c	3	
SMRC parameters		
Gain $w^+ = w^-$	1.5	
LPF cutoff frequency λ_F	10	

For the evaluation of the SMRC, the remainder of the tuning parameters, including constraints and control assumptions, are presented in Table I.

B. Time domain results

First, consider the case where the SMRC mechanism is not employed. In this scenario, the performance of the PT controller structure is analysed considering: (i) a nominal case, without mode uncertainty, and (ii) a 5% uncertainty in the stiffness parameter k_z . The results comparing cases (i) and (ii), over a 20-second interval, are illustrated in Figure 4, where the position, velocity, and force profiles are presented. It can be seen that, due to a small error in the model, the control force exceeds the limit f_{max} (figures 4.e and 4.f), motivating the inclusion of the SMRC method.

Second, consider a PT control, combined with the SMRC mechanism formalised in Section III. Using the parameters from Table I, results in an IMC with $\rho = 1$. Hence, the commutation function is defined as:

$$\sigma = \hat{f}_u - f_u - 10^{-3} f_u^{(1)}. \quad (24)$$

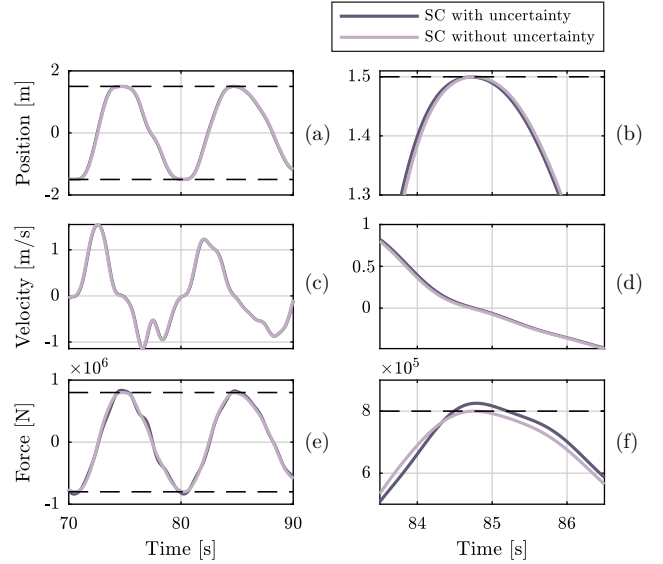


Figure 4. Position, velocity, and force profiles obtained using SC and a PT control loop, without SMRC. (b), (d), and (f), are zoomed regions.

Now, consider case (ii). The results comparing a PT control structure with and without the SMRC mechanism are presented in Figure 5. It can be seen in figures 5.a and 5.b, that the position reference, z^* , is reduced when f_u approaches f_{max} , satisfying the force constraint (Figures 5.e and 5.f). Also, note that both the conditioned and unconditioned velocity profiles (figures 5.c and 5.d) are similar, since the SMRC mechanism is not active if $|f_u + 10^{-3} f_u^{(1)}| < f_{max}$.

Finally, the effects of including the SMRC in a conventional velocity tracking (VT) structure [17] [18], are analysed. To that end, assume the SC provides a velocity reference $v^* = dz^*/dt$.

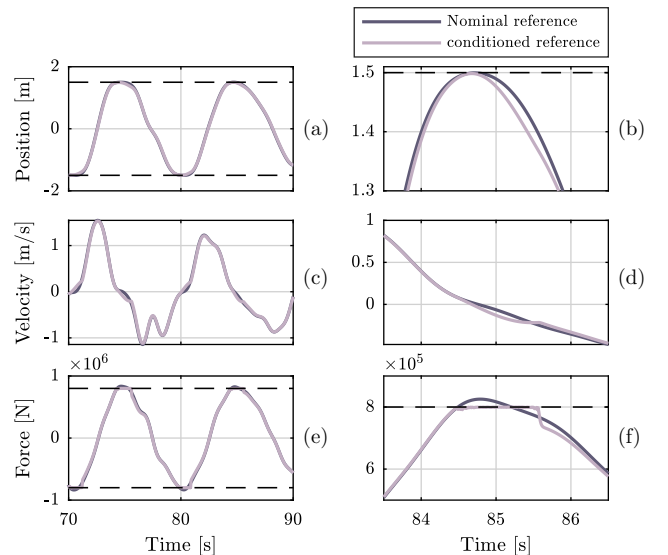


Figure 5. Position, velocity, and force profiles obtained using SC and a PT control loop, including SMRC. (b), (d), and (f), are zoomed regions.

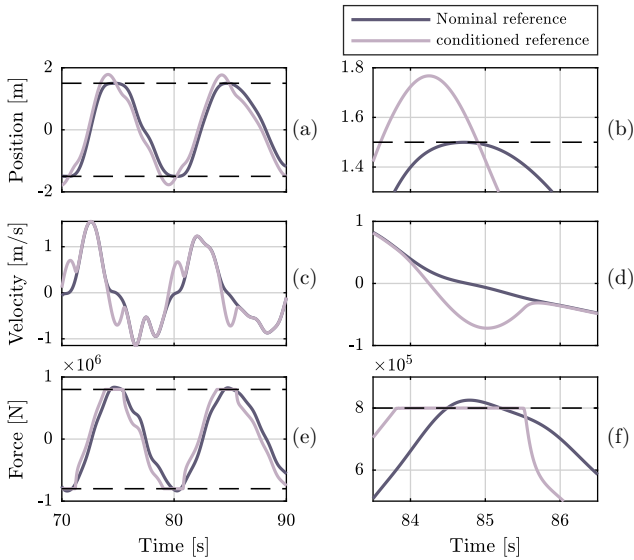


Figure 6. Position, velocity, and force profiles obtained using SC and a VT control loop, including SMRC. (b), (d), and (f), are zoomed regions.

Accordingly, the SMRC is adjusted assuming $\rho = 1$, and using the parameters defined in Table I and (24). The results assuming a 5% uncertainty in the stiffness parameter k_z are presented in Figure 6. It can be appreciated that, similarly to the PT control case, $|f_u| \leq f_{max}$, is effectively satisfied. However, since the conditioned reference is v^* , there is no guarantee of satisfying the position constraints. As can be appreciated in Figure 6.c, the velocity profile is considerably affected when the SMRC is active, leading to larger position values. Indeed, the position surpasses the position constraint by 16%, which is critical for implementation.

V. CONCLUSIONS

In this paper, it is addressed the design of a sliding mode-based reference conditioning mechanism for WEC control strategies, implemented to handle torque/force constraints. To that end, it is considered a position tracking control structure for WECs, and a reference conditioning mechanism is included as an external non-linear control loop, that reduces the position reference when the control effort reaches a design threshold.

The obtained results highlight two fundamental aspects that must be considered in the implementation of closed-loop control for WECs: (i) in the presence of model uncertainty, auxiliary constraint mechanisms are essential, and considering open-loop solutions from optimisation-based controllers is not sufficient to guarantee safe operation; (ii) when implementing a closed-loop control for WECs, considering a position reference is essential, since the results obtained using a velocity reference do not guarantee satisfaction of position constraints. Overall, the methodology presented in this paper is broadly applicable to different tracking structures and could serve as an essential tool for the real-time implementation of control algorithms for WECs. Hence, future work includes real-time testing and validation of the SMRC method in experimental tanks.

ACKNOWLEDGEMENTS

This publication has emanated from research conducted with the financial support of Taighde Éireann – Research Ireland under Grant number 20/US/3776, CONICET, Argentina (PIP 112-2020-0102801CO), UNLP, Argentina (Project I255) and ANPCyT, Argentina (PICT 2018-03747).

REFERENCES

- [1] B. Reguero, I. Losada, and F. Méndez, “A global wave power resource and its seasonal, interannual and long-term variability,” *Applied Energy*, vol. 148, pp. 366–380, Jun. 2015.
- [2] J. V. Ringwood, S. Zhan, and N. Faedo, “Empowering wave energy with control technology: Possibilities and pitfalls,” *Annual Reviews in Control*, vol. 55, pp. 18–44, Apr. 2023.
- [3] N. Faedo, S. Olaya, and J. V. Ringwood, “Optimal control, MPC and MPC-like algorithms for wave energy systems: An overview,” *IFAC Journal of Systems and Control*, vol. 1, pp. 37–56, Sep. 2017.
- [4] D. Garcia-Violini and J. V. Ringwood, “Energy maximising robust control for spectral and pseudospectral methods with application to wave energy systems,” *International Journal of Control*, vol. 94, no. 4, pp. 1102–1113, Jun. 2019.
- [5] N. Faedo, Y. Pena-Sanchez, and J. V. Ringwood, “Receding-horizon energy-maximising optimal control of wave energy systems based on moments,” *IEEE Transactions on Sustainable Energy*, vol. 12, no. 1, pp. 378–386, Jan. 2021.
- [6] N. Faedo, F. D. Mosquera, E. Pasta, G. Papini, Y. Peña-Sanchez, C. A. Evangelista, F. Ferri, J. V. Ringwood, and P. Puleston, “Experimental assessment of combined sliding mode & moment-based control (SM²C) for arrays of wave energy conversion systems,” *Control Engineering Practice*, vol. 144, p. 105818, Mar. 2024.
- [7] F. Fusco and J. V. Ringwood, “A simple and effective real-time controller for wave energy converters,” *IEEE Transactions on Sustainable Energy*, vol. 4, no. 1, pp. 21–30, Jan. 2013.
- [8] N. Faedo, G. Mattiazzo, and J. V. Ringwood, “Robust energy-maximising control of wave energy systems under input uncertainty,” in *2022 European Control Conference (ECC)*. IEEE, Jul. 2022, pp. 614–619.
- [9] P. E. Muñoz, S. A. González, and R. J. Mantz, “Distributed generation contribution to primary frequency control through virtual inertia and damping by reference conditioning,” *Electric Power Systems Research*, vol. 211, p. 108168, Oct. 2022.
- [10] F. Fusco and J. V. Ringwood, “Hierarchical robust control of oscillating wave energy converters with uncertain dynamics,” *IEEE Transactions on Sustainable Energy*, vol. 5, no. 3, pp. 958–966, Jul. 2014.
- [11] J. Falnes and A. Kurniawan, *Ocean Waves And Oscillating Systems: Linear Interactions Including Wave-Energy Extraction*. Cambridge University Press, 2020, vol. 8.
- [12] W. Cummins, “The impulse response function and ship motions,” *Schiffstechnik*, vol. 9, pp. 101–109, 1962.
- [13] T. Pérez and T. I. Fossen, “Time-vs. frequency-domain identification of parametric radiation force models for marine structures at zero speed,” *Model. Identif. Control*, vol. 29, no. 1, pp. 1–19, 2008.
- [14] P. Fornaro, F. D. Mosquera, P. F. Puleston, C. A. Evangelista, and J. V. Ringwood, “Homogeneous filtering unknown input observer for wave energy applications,” in *63rd IEEE Conference on Decision and Control*, Milan, Italy, Dec. 2024.
- [15] C. Edwards and S. Spurgeon, *Sliding mode control: theory and applications*. London: Crc Press, 1998.
- [16] J. H. Todalshaug, G. S. Ásgeirsson, E. Hjalmarsson, J. Maillet, P. Möller, P. Pires, M. Guérinel, and M. Lopes, “Tank testing of an inherently phase-controlled wave energy converter,” *International Journal of Marine Energy*, vol. 15, pp. 68–84, Sep. 2016.
- [17] N. Faedo, U. Bussi, Y. Peña-Sanchez, C. Windt, and J. V. Ringwood, “A simple and effective excitation force estimator for wave energy systems,” *IEEE Transactions on Sustainable Energy*, vol. 13, no. 1, pp. 241–250, Jan. 2022.
- [18] J. V. Ringwood, A. Merigaud, N. Faedo, and F. Fusco, “An analytical and numerical sensitivity and robustness analysis of wave energy control systems,” *IEEE Transactions on Control Systems Technology*, vol. 28, no. 4, pp. 1337–1348, Jul. 2020.